JOURNAL OF FORENSIC SCIENCES

J Forensic Sci, September 2011, Vol. 56, No. 5
doi: 10.1111/j.1556-4029.2011.01819.x
Available online at: onlinelibrary.wiley.com

PAPER

ANTHROPOLOGY

Megan K. Moore,[1] *Ph.D. and Eric Schaefer,*[2] *M.S.*

A Comprehensive Regression Tree to Estimate Body Weight from the Skeleton*,†

ABSTRACT: The purpose of this research is to estimate actual body weight (in particular obesity) from the human skeleton. Known individuals (total $n = 187$) were studied from the Bass Collection from the University of Tennessee, Knoxville. This research combines bone density, cross-sectional geometry of the femur and skeletal pathologies. Bone mineral density was calculated for the proximal femur. Three-dimensional bone surface models were created from computed tomographic scans. Cross-sectional geometry of the femur was calculated at five locations along the diaphysis. The pathologies analyzed were heel spurs, diffuse idiopathic skeletal hyperostosis (DISH), and tibial osteoarthritis. The best regression tree model included only four variables. The first split to estimate body weight was the minimum moment of inertia (I_y) at the distal femur, the second was midshaft width, then anteroposterior thickness at the proximal slice and the final split was the degree of DISH (SD 17.1–31.0 kg). The ability to estimate body weight from the skeleton is one more useful tool for the osteologist.

KEYWORDS: forensic science, forensic anthropology, body mass estimation, femur, cross-sectional geometry, obesity, bone mineral density, computed tomography, osteoarthritis, diffuse idiopathic skeletal hyperostosis

The ability to estimate the extremes of body mass (or weight) from the skeleton represents an intellectual gap in osteological analysis. Previous attempts to estimate body mass account for an average body mass and ignore the body mass extremes of obesity and emaciation. The goal of this research is to explore various biomechanical variables to create a comprehensive predictive model for the estimation of actual body weight and consequently body mass. The body mass index (BMI; kg/m^2) relies on both height and weight. For the sake of simplicity, only body weight in kilograms is estimated in this study.

Three different methodologies are combined in this model: high-resolution computed tomographic (CT) scans, dual-energy X-ray absorptiometry (DEXA), and macroscopic osteological analysis of pathologies. The Bass Donated Skeletal Collection at the University of Tennessee, a large skeletal sample of individuals of known height and weight (among other antemortem data), provides an ideal research scenario to resolve this question. Nondestructive methods of CT and DEXA facilitated analysis of biomechanical and bone mineral density (BMD) properties of the femur, a load-bearing bone of the lower limb. Although these methods may be cost-prohibitive, the thorough approach of this research identifies skeletal modifications that could be adapted for broader range use in both forensics and bioarcheological research.

[1]Department of Behavioral Sciences, University of Michigan—Dearborn, 4901 Evergreen Road, Dearborn, MI 48128.

[2]Penn State Hershey Medical Center, Cancer Institute, 500 University Drive, Hershey, PA 17033.

*Supported by Award No. 2007-DN-BX-0013 awarded by the National Institute of Justice, Office of the Justice Programs, U.S. Department of Justice. The opinions, findings and conclusions expressed in this publication are those of the authors and do not necessarily reflect those of the Department of Justice. Data collection was partially supported by a grant from Center for Musculoskeletal Research.

†Presented at the 78th Annual Meeting of the American Association of Physical Anthropologists, March 31–April 4, 2009, in Chicago, IL.

Received 8 Jan. 2010; and in revised form 5 Aug. 2010; accepted 22 Aug. 2010.

Background Literature

Several biomechanical methods have been proposed for estimating average body mass from the skeleton. These methods are based upon the effects of load bearing and partially on aspects of aging. Load bearing typically affects the lower limb more than the upper; thus, most of the research has focused on this region for body mass estimation. Ruff (1) found significant relationships between body mass and the size of the femoral head. In their study, when one obese subject was included, the prediction error increased to 12–13% for the femoral head and 11% for shaft breadth. This is presumably because the femoral head, being part of a ball and socket joint, has constrained dimensions in adulthood. Lieberman et al. (2) failed to find an increase in the size of articulations of quadrupeds during extensive training. The use of quadrupedal animal models may not translate well to research with bipeds. Eckstein et al. (3) discovered that the joints at the knee were significantly larger in highly active individuals with a history of increased activity. This may correspond to increases in body mass, as obese individuals carry greater loads in daily activities. Porter (4) found a correlation in living individuals between body mass and the width of the ankle, combining the distal tibial and fibular measurements *in vivo*.

Bone density and osteoarthritis (OA) are two variables that could easily be confounded with aging. Body mass has been shown to correlate well with bone density and age (5–7). OA has a strong positive relationship with both body mass and age (8–12). Age will be addressed as a variable considering pathologies and BMD in this study.

Many studies have investigated changing activity patterns because of the ratio of maximum to minimum bending strength in the femoral midshaft. A shape index or I_x/I_y (more precisely

I_{max}/I_{min}) ratio equals the moments of inertia in the direction of greatest bending divided by the moments of inertia in the direction of least bending strength. It has been suggested that a high shape index of the diaphysis has been shown to be the result of greater flexion at the knee (i.e., climbing up stairs or walking over rough terrain) (13–17). Axial compression is most commonly the force of gravity from a person's body mass during standing, walking, or jumping. Ruff and Hayes (18) looked at the relationships between cross-sectional properties and body mass and found significant relationships between all of the variables and body weight, but especially with axial strength.

The biomechanics of obesity varies from a normal gait pattern. Rather than the more pendulous gait seen in normal weight and underweight individuals, obese individuals have a slower, more mediolateral (M–L) saunter (19). As stated earlier, higher anteroposterior (A–P) bending forces are greatest in extreme flexion of the knee, which is rarely observed in obese individuals. The load-bearing elements of the lower limbs of a severely obese individual (BMI > 40) are affected primarily by increased axial loading (from gravity), as when in the stance phase of walking (19–21). The greater axial loading and decreased knee flexion in obese individuals would presumably result in thick and wide femoral cross-sections.

Asymmetry and knee malalignment is a compensatory mechanism in obese individuals, which leads to knee instability and OA (9,21,22). According to several studies, there is an extremely high correlation between obesity and OA with the data from NHANES II and the Framingham study (11,23). One study found a positive "linear" relationship between knee OA and BMI in women (24). Ford et al. (9) found that obese women were 25.1 times more likely to have meniscal tears than normal weight counterparts, a condition that leads to OA. Conversely, OA is almost completely absent in individuals with extremely low bone density and osteoporosis. Dequeker et al. (25) suggested that osteoporosis can *prevent* the development of OA. Both OA and bone density appear to fall along a continuum of body mass, with obesity associated with high bone density and OA on one end, and emaciation associated with osteoporosis and the absence of OA on the other.

The uncertain etiology remains in the clinical literature for the condition called diffuse idiopathic skeletal hyperostosis (DISH) (10,26,27). DISH is a fusion of the vertebrae on the right anterior vertebral bodies, described as being a "candle-wax melting appearance." DISH is considered to be a "diffuse" syndrome, affecting the spine, heels, and other hyperostotic bone growth (10,26,27). Studies have found a correlation of DISH with diabetes mellitus, hyperglycemia, obesity, waist circumference, age, and high-protein diets (10,26–28). A possible etiology could be explained by sit-to-stand studies, in which obese individuals complain of back pain if they are unable to use their arms when standing. Individuals will even avoid leaning forward and use only their quadriceps muscles to stand upright (29). DISH has not been studied extensively in living populations because it is typically asymptomatic. DISH could be the skeletal response to reinforcing stability at the expense of mobility.

All of the previous research on cross-sectional geometry, bone density, and degenerative joint disease individually suggest that obesity will result in a suite of traits. The combination of decreased knee flexion and increased axial compression in ambulatory obese individuals will lead to an increase in cross-sectional area, without an increase in area moments of inertia or torsional strength. Thus, obese individuals would have thick cortical area with a relatively round (A–P = M–L) and narrow shaft diameter for their body mass estimate, if not flattened mediolaterally (M–L > A–P). Greater bone density should be evident because of increased compressive loads. At the other end of the load-bearing spectrum, emaciated individuals will presumably suffer from low bone density (osteopenia), increased fracture risk (osteoporosis), and reduced cortical area. Many factors influence bone density including diet, exercise, body mass, peak bone mass, sex, age, and ancestry. All of these factors also affect body mass, so perhaps this relationship between BMI and BMD is the most important signal. A larger BMI tends to be associated with greater bone density than a smaller BMI (5–7). Lifestyle factors can contribute to osteopenia and osteoporosis in young women and include low body weight, poor nutrition, and various athletic activities (5,30). Female athletes in endurance- or appearance-based sports (e.g., gymnastics, ballet, and running) with reduced calorie diets are more likely to develop early onset osteoporosis (31). The main factors were excessive exercise, low body weight, and amenorrhea. Decreased cortical thickness is another way to evaluate osteoporosis and has been seen in nutritionally stressed populations in Africa and the United States (32,33).

In summary, previous research has focused independently on BMD, cross-sectional geometry, or pathological response to obesity or emaciation. BMD research suggests that larger individuals should have greater bone density and emaciated individuals should have osteoporosis. Studies of the cross-sectional geometry of the femur suggest greater cortical area with increased body mass. Obesity is recognized as a risk factor for OA, for which both conditions are rarely associated with osteoporosis. Diabetes mellitus and high protein diets are highly correlated with the condition DISH of the spine. The current research will tie all of these skeletal responses together in one sample of individuals of known origin to develop a comprehensive model of the effects of body mass on the skeleton to estimate body weight.

Materials and Methods

The research sample consists of modern individuals (total $N = 187$, both men and women combined) from the William M. Bass Donated Skeletal Collection at the University of Tennessee, Knoxville. The Bass Donated Skeletal Collection offers a unique opportunity to study individuals of known age, height, and weight. During the summer of 2005, CT scans were conducted at the University of Tennessee Medical Center with the financial and technical support of the Center for Musculoskeletal Research of the Department of Biomedical Engineering at the University of Tennessee. High-resolution CT scans were collected using a GE Lightspeed 16 Slice CT scanner ($N = 62$ ♀, 94 ♂) (General Electric Healthcare, Waukesha, WI). These DICOM images were manually segmented into three-dimensional (3-D) bone surface models. Ninety of those femora were density (DEXA) scanned at the Department of Exercise, Sport and Leisure Studies at the University of Tennessee ($N = 47$ ♀, 43 ♂). The bones were examined by the first author for skeletal pathologies ($N = 43$ ♀, 82 ♂). The sample number is inconsistent between the CT and the pathologies, because of the fragmentary nature of skeletal remains, even in a controlled setting. Severely fragmented and severe trauma or disease was removed, unless relevant to the study question (e.g., DISH, OA, and heel spurs).

Bone Density Using DEXA

To conduct the density scans, each dry femur was placed in a plastic container that is 65 cm long, 14 cm tall, and 11 cm wide. A 2-cm-thick cube of low-density foam was placed under the lesser trochanter to raise the shaft to be approximately parallel to the table

surface. The distal posterior surface of the condyles was set directly on the bottom of the box. Leveling the femur in this way approximates anatomical position. This method has become standard for this type of research (34) (see Fig. 1). In this study, there was no attempt to rotate the proximal femur to represent more accurately anatomical position. As a result, the lesser trochanter is visible in the density scans, which would not be the case in living individuals.

The bone was placed with the posterior side down on the bottom of the plastic container and the anterior side facing up. The box was filled with dry white rice to a depth of *c.* 12 cm over the proximal end of the bone only, which is a standard method for DEXA bone density analysis. The rice served as a human soft-tissue density equivalent for the DEXA scans, as per the manufacturer of the DEXA Lunar scanner (General Electric Healthcare) and has been used in other studies with success (35) (see Fig. 2). Without the rice, the machine would simply abort the scan. No cover was placed on the plastic container. The box was positioned on the table so that the femur was in approximate anatomical position, as if a patient was lying on the table. In this way, the machine detected a live patient on the table, which facilitated the use of standard DEXA software. The arm of the machine was brought to a level just superior to midshaft. The areas of interest were manually selected on the computer by moving the rectangular field of view over the femoral neck. Two triangular fields of view were placed over the greater and lesser trochanters. Standard measurements of BMD (g/cm^2) were calculated automatically for the femoral neck, Wards triangle, the greater trochanter, proximal shaft, and total BMD. The standard analysis for DEXA bone density measurements of the femur are from the proximal end.

FIG. 1—*Leveling femur for DEXA scan.*

FIG. 2—*Rice as soft tissue equivalent and position on DEXA scanner.*

The DEXA scanner used in this study is located in the Department of Exercise, Sport and Leisure Studies at the University of Tennessee. To standardize the amount of radiation in each scan, the weight of the individual was set to 90 lbs, thus using the "thin mode." This is consistent with a soft-tissue equivalent thickness of 12 cm, suggested by the manufacturer. If we reported a higher body weight, the DEXA machine expected more soft-tissue equivalent material over the bone and would abort the scan. Radiographers sometimes use bags of white rice over extremely lean live subjects in a clinical setting (35). This had no bearing on the results, but maintained a constant level of radiation through the rice and dry bone to ensure a consistent reading from one bone to the next. This aspect of the research is advantageous compared to research with living subjects because when scanning dry bone, the DEXA scanner need not accommodate different tissue thicknesses for obese and emaciated individuals in terms of the amount of radiation as would be the case in living individuals (36). There is a question of the reliability of z-scores; therefore, it is not recommended that the data presented be compared to data from living subjects. A subset of 15 femora was scanned twice to check for intra-observer error. The average measure of intraclass correlation coefficient for the two trials for BMD at all locations was 0.99 (α level $p = 0.00$).

Osteological Analysis of Pathologies

Each skeleton was analyzed for all pathologies. This was conducted blindly from the knowledge of body mass information. DISH is considered to be a "diffuse" syndrome on the spine, with spicules on the heels other hyperostotic bone growth on the skeleton (i.e., pelvis, humerus) (10,26,27). Only the spinal manifestation and heel spurs were recorded in this study. The presence of the vertebral trait of DISH was recorded if three or more vertebrae were fused along the anterior right side of the vertebral bodies and only if disk space was preserved. A note was made on the severity of the manifestation and which vertebrae were involved. Heel spurs were scored from zero to three based on the severity of the heel spur. Only those heel spurs on the inferior surface of the calcaneous were recorded.

There can be a significant amount of inter-observer error when scoring for arthritis, but the analysis of large samples can give a reasonable approximation (10). Bridges (37) and Ortner (38) recommend providing as much detail as possible. The scoring procedure utilized here was consistent with Bridges (39), but the slight and mild categories were collapsed, to have only scores of zero to three (e.g., 0 = absent, 1 = trace, 2 = moderate, 3 = severe). OA was scored for variations in severity and location. Three locations on the skeleton were the focus in this study. Both right and left sides were scored when possible, and the tibial plateau was divided into medial and lateral condyles to record them separately. The femoral head was also scored for OA. The scoring for this variable was broken down into lipping, extent of lipping, porosity, eburnation, and extent of eburnation. The extent of lipping and eburnation were defined as the proportion of the circumference of the articulation affected, from zero to three. A score of two, for example, was

recorded when two-thirds of the tibial condyle exhibited lipping. Porosity proved to be a more arbitrary designation and did not correspond well with eburnation or lipping, as there may be signs of porosity as a result of bone deposition or resorption.

CT Scanning, Cross-sectional Geometry, and 3-D Model Creation

CT is superior to magnetic resonance and ultrasound for imaging of a skeleton. This is because CT performs multiple 2-D slices of 3-D objects and mathematically reconstructs the cross-sectional image from the X-ray measurement of thin slices (40). In essence, the CT creates 3-D radiographs. The advantages of CT data are numerous: rapid data acquisition, it is relatively nondestructive (with some possible DNA degradation [41]), and it provides high-resolution 3-D data of both internal and external bone surfaces and information on bone density.

In conjunction with a team of biomedical engineers and anthropologists, CT scans were conducted on the skeletal remains of individuals from the William M. Bass Skeletal Collection. To facilitate rapid data collection, six identical sets of two boxes lined with low-density foam were constructed. The position of the boxes was standardized in the CT scanner by strapping a board to the scanner table.

Through the process of segmentation of the DICOM images, the internal and external bone surfaces were recognized, the data were interpolated between slices, and the surfaces were smoothed through a series of iterations using the computer software program AMIRA (Visage Imaging, San Diego, CA) (42,43) (see Fig. 3). An atlas was developed from an averaging of the many different femoral models and programmed in MATLAB (The MathWorks Inc., Natick, MA). The atlas is necessary for the automation because it recognizes the anatomical orientation of the bone and major axes. Thousands of homologous points can be identified with the overlay of a superficial triangular mesh. Further, it permits mirroring of the bones to analyze all bones as the right side (42,44).

A second algorithm was written, designed after the program SLICE (45) to calculate the moments of inertia and biomechanical properties. The "ideal" axis was calculated and corresponds to the straight axis from the midpoint of the distal articulation to the cervical axis at the proximal end of the shaft. This serves as the *z*-axis of the femur, with the more positive z being proximal. The M–L direction served as the *x*-axis with the more positive x being lateral. The *y*-axis corresponds to the A–P direction being more positive anteriorly. The *xz* plane refers to the frontal plane, the *yz* to the sagittal plane, and the *xy* to the transverse plane. The middle 60% is typically used in this type of analysis because the distal ends of the femoral shaft consist of a significant amount of trabecular bone changing the macrostructural properties of the bone. Transverse cross-sections were analyzed at five locations perpendicular to the femoral shaft: 80%, 65%, 50%, 35%, and 20%. The 80% position is the most proximal cross-section and the 20% the most distal (see Fig. 4). Table 1 provides a list of all of the cross-sectional geometry variables used initially.

The moments of inertia are length measurements from the area of the centroid to the outer perimeter of the bone. The second moment of inertia (I_x) in the M–L direction is perpendicular to the I_y direction, which runs A–P. The second moments of area about the principal axes are the directions of maximum and minimum bending strength, with the greatest distance from the centroid (I_{max}), which is perpendicular to the minimum second moment of inertia (I_{min}). By taking these principal second moments and dividing the I_{max} by the I_{min}, we arrive at a shape index, in which size has been removed. This same equation can be applied to the second moments of inertia in the A–P and M–L directions. The reliability of the measurements was compared to the inter-observer error between five anthropologists. The results showed much lower variation (<0.95) than between the five anthropologists.

For the statistical analysis, the most significant covariates of body mass (bone density, cross-sectional area, OA, DISH, and heel spurs) were selected and combined into a regression tree using the statistical software "R" (R Foundation for Statistical Computing, Vienna, Austria). The variable selection method of McHenry's Algorithm comes standard in the statistical package NCSS 1997 (Number Cruncher Statistical Systems, Kaysville, UT). McHenry's algorithm first finds the best variable based on the highest *R*-squared value, then the best pair of variables, and so on. The data were divided into each data collection method (density, pathology, and cross-sectional geometry) to first select the best variables using McHenry's variable selection (46) available on NCSS. The best variable of each research method was then subjected to a second variable selection to choose the best variables overall. This method may not account for some unforeseen interactions between methodologies, but it was a way to reduce the data and the variables selected mostly coincided with the initial hypothesis. The variable selection method reduced the overall number of more than 100 variables down to only 17 variables listed in Table 2. The regression tree will serve to demonstrate the relationships between the categorical variables to develop a predictive model for estimating body weight.

To emphasize the relationship between the pathological variables and body mass, the pathological data were analyzed independently using logistic regression. The dummy variables of obese (BMI > 30) or not obese were used. Ordinal pathology variables were collapsed into present or absent. Age as a category was broken down into two dichotomous variables: older age as above 55 years and younger age as below 55. Logistic regression was calculated for each sex individually and the sexes pooled.

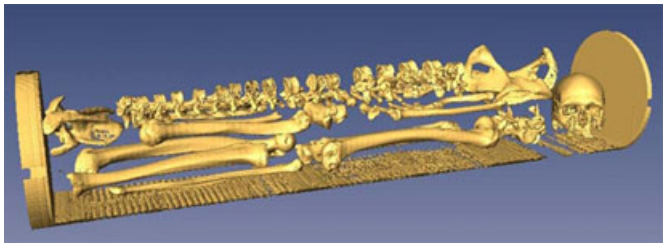

FIG. 3—*Automatic segmention of a skeleton.*

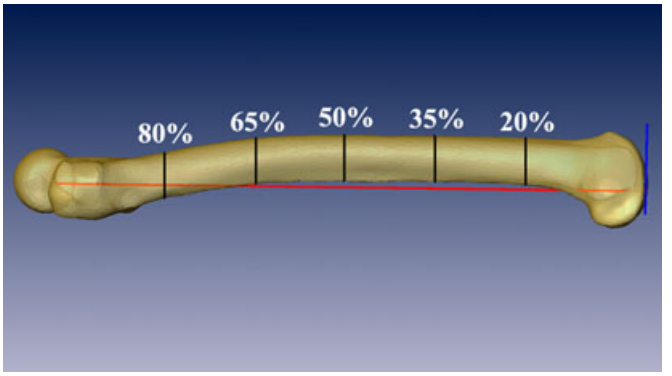

FIG. 4—*Five femoral cross-sections along the anatomical axis.*

TABLE 1—*Cross-sectional geometry variables.*

Total cross-sectional area
Cross-sectional area of cortical bone
Cross-sectional area of medullary canal
Second moments of inertia I_x and I_y perpendicular through centroid—I_x for mediolateral direction, I_y for anteroposterior direction
Product of inertia about *x*- and *y*-axes translated to centroid
Second moments of inertia about principal axes (I_{max} and I_{min})
Angle between translated *x*- and *y*-axes and principal axes
Maximum distance along major axis from area of centroid to outer perimeter
Maximum distance along minor axis from area of centroid to outer perimeter
Polar moment of area = J → approximating torsional rigidity
Centroid—center of cortical area

TABLE 2—*Variables selected using McHenry's algorithm.*

General	Bone Density	Cross-Sectional Geometry	Skeletal Pathology
Height	Neck BMD	I_y at 20%	Presence of heel spur
Age	Wards BMD	I_y at 50%	DISH (present, mild, and absent)
		I_y at 65%	M–L width of proximal right tibia
		I_y at 80%	OA of left medial tibia
		J at 80%	
		F_B_50%	
		F_B_65%	
		F_A_80%	
		Total AREA at 80%	
		I_{max}/I_{min} at 50%	

BMD, bone mineral density; DISH, diffuse idiopathic skeletal hyperostosis; M–L, mediolateral; OA, osteoarthritis.

The benefit of using a regression tree is the method for which missing variables are accounted. The regression tree recognizes the greatest signal as the first split. The regression tree automatically creates meaningful divisions within the data. Standard regression models, such as linear or logistic regression, can easily accommodate both categorical and continuous parameters. The regression tree is a special type of regression model that can also handle both types of parameters. Advantages of the regression tree compared to standard regression approaches are that continuous variables do not enter the model linearly, and cut points for all variables are not prespecified, but driven by the data. Our goal was to predict weight (in kg) based on the femur measurements and other data collected. We had two difficulties in accomplishing this goal. First, there was an exceedingly large number of possible predictors. Second, many variables had missing values, some with as much as 40% missing. To accommodate the first difficulty, we restricted our set of possible predictors to the 17 variables identified in the principal variable analysis. To accommodate the second difficulty, we used a regression tree, which handled missing data without simply removing incomplete observations. In addition, the tree allowed for modeling complex relationships among predictors, and offered a straightforward interpretation.

The regression tree was built using RPART (47) in the software package R. The tree was initially built by determining the single numeric split of any predictor that resulted in the largest reduction in variance of weight compared to all splits in all other predictors. The data were then split into two subgroups. Within each subgroup, the process was repeated in the same fashion and recursively continued within each resulting subgroup until no improvement in variance could be made. The final terminal nodes of the tree were summarized by the mean weight, with the minimum, maximum, and variance also provided. During construction of the tree, when a variable to be split contained missing values, the RPART algorithm was re-applied to predict the split by finding the optimal split in all other independent variables. The optimal split with the highest agreement to the original split with missing values was then used to classify missing observations.

Cross-validation was used to select the final tree and guard against overfitting to our particular sample of data. Cross-validation is a general statistical approach used to validate regression models and does not imply that a formal discriminant function analysis (DA) was conducted, although the regression tree is a (more sophisticated) cousin to DA. Cross-validation for the regression tree was performed as per the authors of the software. The purpose of cross-validation was to reduce the original regression tree, which had a large number of nodes and was overfit to our particular data (e.g., too complex), to a smaller tree with fewer nodes that is more likely to accurately predict responses on future subjects not used to develop the model. The smaller tree selected by cross-validation is reported elsewhere.

Results

Only the collapsed dummy variables of present and absent and obese versus not obese were used for the logistic regression (obese = BMI > 30). The odds ratios for women for DISH, heel spurs, and all locations of OA had significant Wald probabilities. The odds ratios ranged from 5.1 for heel spurs, 9.9 for DISH, and 23.9 for left medial OA. For men, the odds ratios were not significant for heel spurs, left lateral OA, or right lateral OA. Only men showed significant odds ratios for DISH of 6.5, and for the right and left medial tibial plateaus, 4.4 and 15.5, respectively. When pooling the sexes, all OA sites had significant odds ratios ranging from 3.6 to 7.9, with the most severe for the left medial OA, DISH, and then right medial OA. When comparing age as the dependent variable rather than weight, only DISH and OA of the right medial tibia were significant with odds ratios >3.8 (see Table 3).

The final regression tree was chosen using the 1-SE rule (47), which stipulated that, among those trees within one standard error of the minimum cross-validated risk, the tree with the fewest splits should be chosen. The results are summarized in Fig. 5. The first division splits the data for the variable of the second moment of inertia in the A–P direction at the most distal 20% slice. If the I_y variable at this slice was >3.98 cm^4, then the estimated weight of the individual is 56.79 kg ± 17.1. From that node, if the I_y variable was greater than 3.98 cm^4, the next split was determined by the distance from the subperiosteal surface of the bone to the centroid in the M–L direction at the level of the femoral midshaft. If greater than 1.495 cm, the average weight for this terminal node is 115.2 kg ± 31.0. If this breadth measurement is >1.495 cm, then the next split is between the A–P distance from the external subperiosteal surface to the centroid at the 80% slice or the most proximal slice of the bone. If this distance is >1.685 cm, the average weight for this terminal node is 76.77 kg ± 19.3. If greater than 1.685 cm, the next split is dependent on the severity of the condition DISH. This was scored as none = 0, 0.5 = mild, and severe = 1.0. For those cases of mild-to-no DISH, the mean weight for the terminal node is 84.46 kg ± 18.2. If the DISH is severe, the estimated weight of the individual is 115.5 kg ± 31.3. The overall R^2 value is 0.44, which means that 44% of the variation in weight is explained by the regression tree. There were three outliers in this

TABLE 3—*Logistic regression odds ratios for women, men, sexes pooled, and for age as dependent.*

Pathology	*N*	Odds Ratio	*p*-Value
Women			
DISH	40	9.900	0.003*
Heel spur	38	5.066	0.027*
OA tibia left lateral	38	6.999	0.017*
OA tibia left medial	39	23.999	0.006*
OA tibia right lateral	40	5.499	0.025*
OA tibia right medial	40	5.600	0.019*
Men			
DISH	53	6.417	0.004*
Heel spur	51	2.700	0.127
OA tibia left lateral	53	2.679	0.186
OA tibia left medial	53	4.375	0.037*
OA tibia right lateral	50	3.333	0.133
OA tibia right medial	50	15.500	0.016*
Sexes pooled			
DISH	93	7.692	0.000*
Heel spur	89	3.594	0.008*
OA tibia left lateral	91	4.163	0.008*
OA tibia left medial	92	7.958	0.000*
OA tibia right lateral	90	4.082	0.009*
OA tibia right medial	90	6.741	0.001*
Sexes pooled age as dependent			
DISH	90	3.041	0.027*
Heel spur	86	1.653	0.302
OA tibia left lateral	88	2.667	0.086
OA tibia left medial	89	2.358	0.135
OA tibia right lateral	88	2.284	0.151
OA tibia right medial	88	3.770	0.029*

*$p < 0.05$.
DISH, diffuse idiopathic skeletal hyperostosis; OA, osteoarthritis.

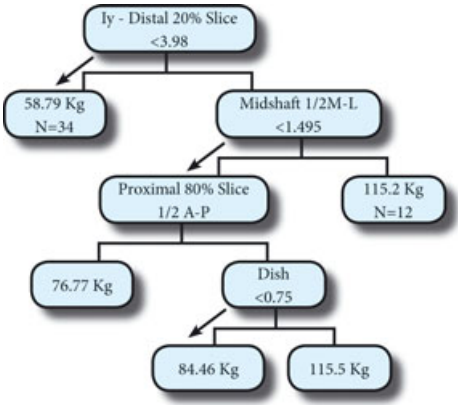

FIG. 5—*Decision tree to estimate body weight from the skeleton.*

model, and the greatest standard deviation was for the individuals with a mean body weight of *c.* 115 kg. When comparing this value to height, body weight increased *c.* 1 kg for every 1 cm of height increase.

Discussion and Conclusion

From this research, we can conclude that it is possible to estimate modern human body mass from the skeleton, including the extremes of both emaciation and obesity. Of the measures selected in this regression tree, the nodes selected show an overall M–L widening of the shaft at the proximal, distal, and midshaft of the femur for individuals greater than 115 kg. This body weight would be considered obese for anyone below 1.95 meters in height or well over six feet tall. The results of this study are consistent with those from logistic regressions using single variables (Table 3). Obese individuals were between seven and eight times more likely to have OA of the right and left medial tibiae, respectively, and nearly eight times more likely to have DISH in the spine. DISH is not understood clinically because it is asymptomatic and often is not evident on radiographs. DISH is often thought to be more frequent in men than in women clinically. In this skeletal sample, however, 43% of men and 41% of women exhibit moderate to severe DISH. As for BMD, in both sexes, there was a stronger correlation with BMD and BMI, than for age. Obesity plays a greater role in the etiology of these degenerative diseases than does aging. Some traits show a greater relationship with body weight and body mass, but by identifying the distribution pattern of these traits on the skeleton, we can distinguish random trauma from the combined effects of excessive body mass.

Most of the variables used in this regression tree can be adapted for measurement using calipers, except for the first and most significant split. Thus, the feasibility of broad use of this method broadly is reduced. Calipers were not used initially so that all of the possible morphological and pathological alterations could be recognized using the robust statistical methods and 3-D computer modeling. This was a crucial first step in recognizing the most important signals. Future research will begin to look only at external measurements of the bones of the proximal and distal M–L widths of the femur. A recent study by Agostini (48) corroborates these findings concerning changes in shape of the femur. She found a significant increase in M–L width of the proximal and midshaft of the femur in overweight individuals using external measurements of 184 men of European ancestry.

The findings in this study do not support the original hypothesis that cross-sectional area and BMD will have the highest correlation with body mass and body weight. Rather, the width measures at the distal and proximal ends of the femur and DISH are selected as the most significant signal. It was predicted that the cross-sectional area of the midshaft would be most significant, when in fact the most distal slice of the femur had the greatest signal. We did not find a clear relationship between cross-sectional shape (I_{max}/I_{min} or I_y/I_x) and obesity. This could either be because of the fact that activity patterns were not consistent with variation with body weight or that the shape index does not truly express activity as has been suggested. Some width and length measures appear to be individually more reflective of body weight. The individual moment of inertia in the A–P direction at the most distal cross-section on the shaft appears to best reflect changes in body weight. This could be reflecting what Ford et al. (9) wrote about strain and torque increasing in obese leading to a higher risk of injury. There was no evidence of a decrease in the canal size in obese individuals, which does not support endosteal apposition in adulthood the hypothesis. In a preliminary study (49), this was found to be the case in a sample of 24 women, looking at cross-sectional area of the femoral waist (least circumference). Perhaps this location is more important biomechanically than the midshaft, or the results of the previous study were reflecting sampling error.

The lowest bone density was found in emaciated individuals and the highest bone density in the obese individuals; however, the signal was not great enough to be included in this regression tree model. When comparing the different female BMI categories using analysis of variance, the results were significant ($p < 0.05$) at all locations between the emaciated and obese and between emaciated and average reported elsewhere (43). When comparing obese to average weight individuals, there were no significant differences. For men, the results were nearly the same as those reported in a

previous publication (43). This relationship may reflect the change in the gait of severely obese individuals from an anterior to posterior swing of the legs to a more M–L saunter. This change in gait pattern widens the proximal femoral shaft in this M–L direction, changing the shape of the shaft near the hip, causing a reconfiguring of the bone geometry at the knee, as well.

One benefit of this study is the combination of multiple indicators to provide evidence of a suite of traits. We hope that this study encourages other researchers to examine body weight/mass estimation utilizing a more holistic perspective.

The William M. Bass Donated Skeletal Collection provides an unparalleled opportunity to explore this secular change in body mass. This large sample of modern individuals of known height and weight reflects the broad spectrum of human body mass from a BMI of 11 to 88. By using a skeletal sample, we can visualize changes on the skeleton that are unclear on radiographs and asymptomatic (e.g., DISH). A skeletal sample also permits the conduction of high-resolution CT scans that would expose living subjects to excessive amounts of radiation. This research presents just one application of 3-D computer models, but there are an infinite number of ways to take advantage of this technology. These models, when added to a bone atlas, can be used to automatically quantify shape. This method is similar to those geometric morphometric methods used on the skull. Instead of a few dozen discrete landmarks, the 3-D femoral models used here have 7500 evenly distributed points. Another benefit of using skeletal material is the ability to standardize tissue depths with the DEXA scans. One problem with DEXA is the error involved when scanning through large amounts of soft-tissue in obese individuals. The method developed uses bones from a wide range of body mass indices, but with the same depth of soft-tissue equivalent. Thus, any differences will reflect the actual density and not error in accounting for soft tissues.

There are several drawbacks in these methodologies. This method is clearly not feasible for every researcher. This is, however, an important first step toward body weight/mass estimation that can account for the extremes of body weight. Owing to the smaller sample size, men and women were combined in the overall estimations. The rational is that these skeletal manifestations are the result of the environment and ''weight'' and not as the result of genetic factors. There are sex differences in gait, but we are emphasizing that the skeletal accommodations to obesity are similar. Furthermore, DEXA has become the gold standard with bone density research, and this allows comparisons with the clinical literature. To estimate body weight in this study, the most significant variable is the moment of inertia in the A–P direction and requires analysis of the femoral cross-section. This can be accomplished by destructive analysis of cutting the bone or by nondestructive CT. In the past, CT has been relatively cost-prohibitive, but this too is changing and the technology is readily available in most clinics and hospitals. As there are many confounding factors in the literature concerning the effects of juvenile obesity, this is an increasingly important area of future research. At present, there is little research concerning how obesity affects the juvenile or adolescent skeleton.

Osteologists possess a set of skills to reveal the biological profile from human skeletal remains. The osteologist can estimate the age at death, sex, stature, and ancestry of a skeleton with a high-to-moderate degree of accuracy. Body mass/weight would provide a useful addition to skeletal analysis, but current methods typically center on average body mass, disregarding the extremes of emaciation and obesity. This becomes particularly apropos today, when it is estimated that 32.2% of the American adult population is obese (50). The ability to estimate body weight extremes would be a valuable addition to the biological profile for forensic analysis to achieve individuation of a skeleton. It could be useful to determine whether obesity existed prehistorically in a particular segment of the population.

Acknowledgments

This research could not have been completed without the expertise of the Biomedical Engineers of the University of Tennessee under the direction of Dr. Mohamed Mahfouz. We acknowledge the invaluable advice and support of Dr. Lyle Konigsberg and Dr. Richard Jantz on this project. Many thanks to Dr. Kent Hutson of the UT Medical Center for facilitating the CT scans and technical advice. Thanks to Dr. Dixie Thompson of the Department of Exercise, Sport and Leisure Studies at UT, who collaborated with the bone density scans and permitted use of DEXA. Thanks are due to Dr. Lee Meadows Jantz for her help and permission to use the William M. Bass Donated Collection. The following Biomedical Engineers provided their technical expertise, without which, this work could not have been completed: Emam ElHak Ali Abd ElFatah, Brandon Merkl, Mike Kuhn, and Katherine Kesler. We thank the following individuals for helping with the CT scanning: Jenn Lilly, Donna McCarthy, Amanda Allbright, Emily Loucks, Rebecca Wilson, Elizabeth DiGangi, Anne Kroman, Lorena Villao, Katie King, Brian Pope, Genevieve Ritchie, Kate Driscoll, Courtney Eleazer, Kanchana Jagannathan, and the CT Tech, Todd Malone.

References

1. Ruff CB. Climate, body size and body shape in hominid evolution. J Human Evol 1991;21:81–105.
2. Lieberman DE, Devlin MJ, Pearson OM. Articular area responses to mechanical loading: effects of exercise, age, and skeletal location. Am J Phys Anthropol 2001;116(4):266–77.
3. Eckstein F, Faber S, Mühlbauer R, Hohe J, Englmeier K-H, Reiser M, et al. Functional adaptation of human joints to mechanical stimuli. Osteoarthritis Cartilage 2002;10(1):44–50.
4. Porter AMW. The prediction of physique from the skeleton. Int J Osteoarchaeol 1999;9:102–15.
5. Gibson JH, Mitchell A, Harries NG, Reeve J. Nutritional and exercise-related determinants of bone density in elite female runners. Osteoporos Int 2004;15:611–8.
6. Miyabara Y, Onoe Y, Harada A, Kuroda T, Sasaki S, Ohta H. Effect of physical activity and nutrition on bone mineral density in young Japanese women. J Bone Miner Metab 2007;25:414–8.
7. Wheatley BP. An evaluation of sex and body weight determination from the proximal femur using DXA technology and its potential for forensic anthropology. Forensic Sci Int 2005;147:141–5.
8. Coggon D, Reading I, Croft P, McLaren M, Barrett D, Cooper C. Knee osteoarthritis and obesity. Int J Obes 2001;25:622–7.
9. Ford FM, Hegmann KT, White GL, Holmes EB. Associations of body mass index with meniscal tears. Am J Prev Med 2005;28(4):364–8.
10. Moskowitz RW. Clinical and laboratory findings in osteoarthritis. In: McCarty DJ, Koopman WJ, editors. Arthritis and allied conditions: a textbook of rheumatology, 12th edn. Philadelphia, PA: Lea and Febiger, 1993;1735–59.
11. Sharma L, Kapoor D, Issa S. Epidemiology of osteoarthritis: an update. Curr Opin Rheumatol 2006;18:147–56.
12. Stürmer T, Günther K-P, Brenner H. Obesity, overweight and patterns of osteoarthritis: the Ulm Osteoarthritis Study. J Clin Epidemiol 2000; 53:307–13.
13. Larsen CS. Bioarchaeology: interpreting behavior from the human skeleton. Cambridge, MA: Cambridge University Press, 1997.
14. Lovejoy CO, Burstein AH, Heiple KG. The biomechanical analysis of bone strength: a method and its application to platycnemia. Am J Phys Anthropol 1976;44:489–506.
15. Ruff CB. Sexual dimorphism in human lower limb bone structure: relationship to subsistence strategy and sexual division of labor. J Human Evol 1987;16:391–416.

16. Ruff CB, Hayes WC. Cross-sectional geometry of pecos pueblo femora and tibiae—a biomechaical investigation: I. Method and general patterns of variation. Am J Phys Anthropol 1983;60:359–81.
17. Ruff CB, Hayes WC. Bone mineral content in the lower limb: relationship to cross-sectional geometry. J Bone Joint Surg 1984;66A:1024–31.
18. Ruff CB. Body mass prediction from skeletal frame size in elite athletes. Am J Phys Anthropol 2000;113:507–17.
19. Hills AP, Hennig EM, Byrne NM, Steele JR. The biomechanics of adiposity-structural and functional limitations of obesity and implications for movement. Obes Rev 2002;3:35–43.
20. Syed IY, Davis BL. Obesity and osteoarthritis of the knee: hypotheses concerning the relationship between ground reaction forces and quadriceps fatigue in long-duration walking. Med Hypotheses 2000;54(2):182–5.
21. Messier SP, Ettinger WH Jr, Doyle TE, Morgan T, James MK, O'Toole ML, et al. Obesity: effects on gait in an osteoarthritic population. J Appl Biomech 1996;12:161–72.
22. Sharma L, Lou C, Cahue S, Dunlop DD. The mechanism of the effect of obesity in knee osteoarthritis: the mediating role of malalignment. Arthritis Rheum 2000;43(3):568–75.
23. Felson DT, Hannan MT, Naimark A, Berkeley J, Gordon G, Wilson PWF, et al. Occupational physical demands, knee bending, and knee osteoarthritis: results from the Framingham study. J Rheumatol 1991;18:1587–92.
24. Mannienen P, Riihimäki H, Heliövaara M, Mäkelä P. Short communication: overweight, gender, and knee osteoarthritis. Int J Obes 1996;20:595–7.
25. Dequeker J, Goris P, Uytterhoeven R. Osteoporosis and osteoarthritis (osteoarthrosis): anthropometric distinctions. J Am Med Assoc 1983;249(11):1448–51.
26. Mader R, Sarzi-Puttini P, Atzeni F, Olivieri I, Pappone N, Verlaan JJ, et al. Extraspinal manifestations of diffuse idiopathic skeletal hyperostosis. Rheumatology 2009;48(12):1478–81.
27. Jankauskas R. The incidence of diffuse idiopathic skeletal hyperostosis and social status correlations in Lithuanian skeletal materials. Int J Osteoarchaeol 2003;13:289–93.
28. Patrick PJ. Greed, gluttony and intemperance? Testing the stereotype of the 'Obese Medieval Monk' [PhD Thesis]. London (UK): University of London, 2005.
29. Galli M, Crivellini M, Sibella F, Montesano A, Bertocco P, Parisio C. Sit-to-stand movement analysis in obese subjects. J Obes Relat Metab Disord 2000;24(11):1488–92.
30. Reid IR. Relationships between fat and bone. Osteoporos Int 2007;19(5):595–606.
31. Ridout CF. Old bones in young bodies. Am Fitness 1999;14(5):28.
32. Hummert JR. Cortical bone growth and dietary stress among subadults from Nubia's Batn El Hajar. Am J Phys Anthropol 1983;62:167–76.
33. Martin DL, Magennis AL, Rose JC. Cortical bone maintenance in an historic Afro-American cemetery sample from Cedar Grove, Arkansas. Am J Phys Anthropol 1987;74:255–64.
34. Ruff CB. Structural changes in the lower limb bones with aging at Pecos Pueblo [PhD Thesis]. Philadelphia (PA): University of Pennsylvania, 1981.
35. Haigh C. Estimating osteological health in Ancient Egyptian bone via applications of modern radiological technology. Assemblage: The Sheffield Graduate Journal of Archaeology 2000, http://ads.ahds.ac.uk/catalogue/adsdata/assemblage/html/5/haigh.html#state (accessed May 13, 2011).
36. Steinschneider M, Hagag P, Rapoport MJ, Weiss M. Discordant effect of body mass index on bone mineral density and speed of sound. BMC Musculoskelet Disord 2003;4:15.
37. Bridges PS. Changes in long bone structure with the transition to agriculture: implications for prehistoric activities [PhD Thesis]. Ann Arbor (MI): University of Michigan, 1985.
38. Ortner DJ. Identification of pathological conditions in human skeletal remains, 2nd edn. Amsterdam, The Netherlands: Academic Press, 2003.
39. Bridges PS. Degenerative joint disease in hunter-gatherers and agriculturalists from the southeastern United States. Am J Phys Anthropol 1991;85(4):379–91.
40. Brant WE. Diagnostic imaging methods. In: Brant W, Helms C, editors. Fundamentals of diagnostic radiology. Baltimore, MD: Williams and Wilkins Pub, 1994;3–24.
41. Hall EJ. Radiation biology for pediatric radiologists. Pediatr Radiol 2009;39(Suppl. 1):S57–64.
42. Mahfouz MR, Merkl B, Abdel Fatah EE, Booth R Jr, Argenson JN. Automatic methods for characterization of sexual dimorphism of adult femora: distal femur. Comput Methods Biomech Biomed Engin 2007;10:447–56.
43. Moore MK. Body mass estimation from the human skeleton [PhD dissertation]. Knoxville (TN): University of Tennessee, 2008.
44. Mahfouz MR, Badawi A, Merkl B, Abdel Fatah EE, Pritchard E, Kesler K, et al. Patella sex determination by 3D statistical shape models and nonlinear classifiers. Forensic Sci Int 2007;173:161–70.
45. Nagurka ML, Hayes WC. An interactive graphics package for calculating cross-sectional properties of complex shapes. J Biomech 1980;13:59–64.
46. McHenry C. Multivariate subset selection. J R Stat Soc Series C 1978;27:291–6.
47. Therneau TM, Atkinson EJ. An introduction to recursive partitioning using the RPART routines. Rochester, MN: Section of Biostatistics, Mayo Clinic, Technical Report Series No. 61, 1997, Nov.
48. Agostini GM. The impact of obesity on the morphology of the femur. Proceedings of the 62nd Annual Meeting of the American Academy of Forensic Sciences; 2010 Feb 22–27; Seattle, WA. Colorado Springs, CO: American Academy of Forensic Sciences, 2010;402.
49. Moore M, Fatah EA, Mahfouz M. Body mass estimation from human femoral midshaft cross-sectional area. Supplement: Proceedings of the Seventy-Sixth Annual Meeting of the American Association of Physical Anthropologists; 2007 Mar 28–31; Philadelphia, PA. Malden, MA: American Association of Physical Anthropologists 2007;132(S44):173–4.
50. Ogden CL, Carroll MD, Curtin LR, McDowell MA, Tabak CJ, Flegal K. Prevalence of overweight and obesity in the United States, 1999–2004. J Am Med Assoc 2006;295(13):1549–55.

Additional information and reprint requests:
Megan K. Moore, Ph.D.
Assistant Professor of Anthropology
Department of Behavioral Sciences
University of Michigan—Dearborn
4901 Evergreen Road
Dearborn, MI 48128
E-mail: mooremeg@umd.umich.edu